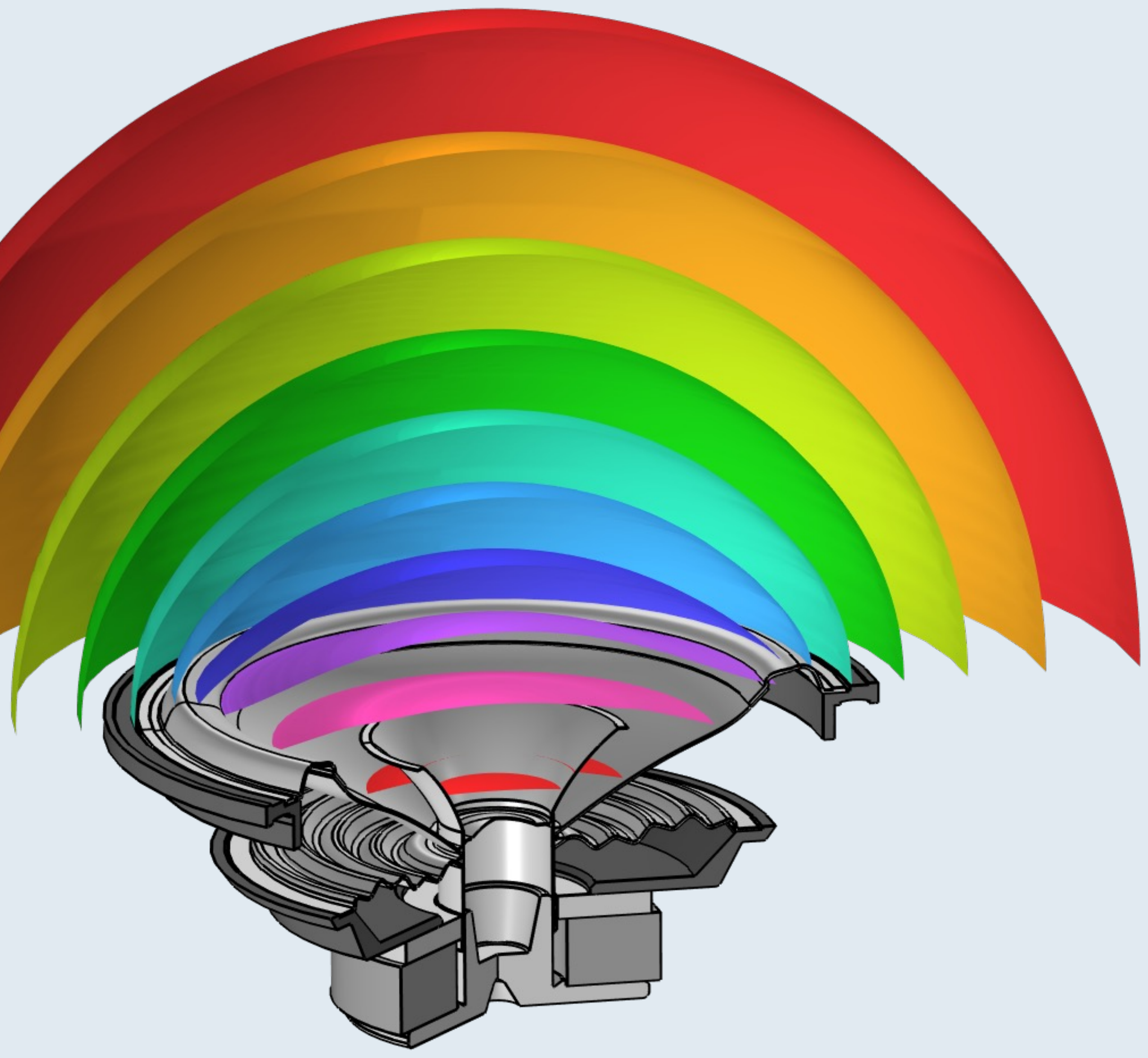

Advanced FEM Simulation of Dynamic Loudspeaker Performance: The Impact of Cone and Surround Materials

Accurately understanding and modeling material variations is crucial for FEM simulations in loudspeaker design, as small changes in material properties can greatly affect performance.

A. Replogle[1,2], C. Corsini[2], L. Villa[2]
1. Politecnico di Milano, Milan, Italy.
2. R&D, Faital S.p.A., Milan, Italy.

Abstract

Finite Element Method (FEM) simulations offer a powerful tool for optimizing loudspeaker designs. This work focuses on the important role of material selection, analyzing how different cone and surround materials influence loudspeaker acoustic performance. The study involved material characterization through physical testing and simulations, with materials tested including loudspeaker cones: paper, fiberglass, paper + Kevlar, paper + mica, and for surrounds: rubber, cloth, and foam.

By analyzing material properties like Young's modulus and density, the study provides valuable insights into material characteristics for improving loudspeaker design strategies and enhancing overall sound quality. Comparisons between the simulated and measured frequency response and impedance curves validated the accuracy of loudspeaker models, demonstrating the importance of precise material inputs in FEM simulations.

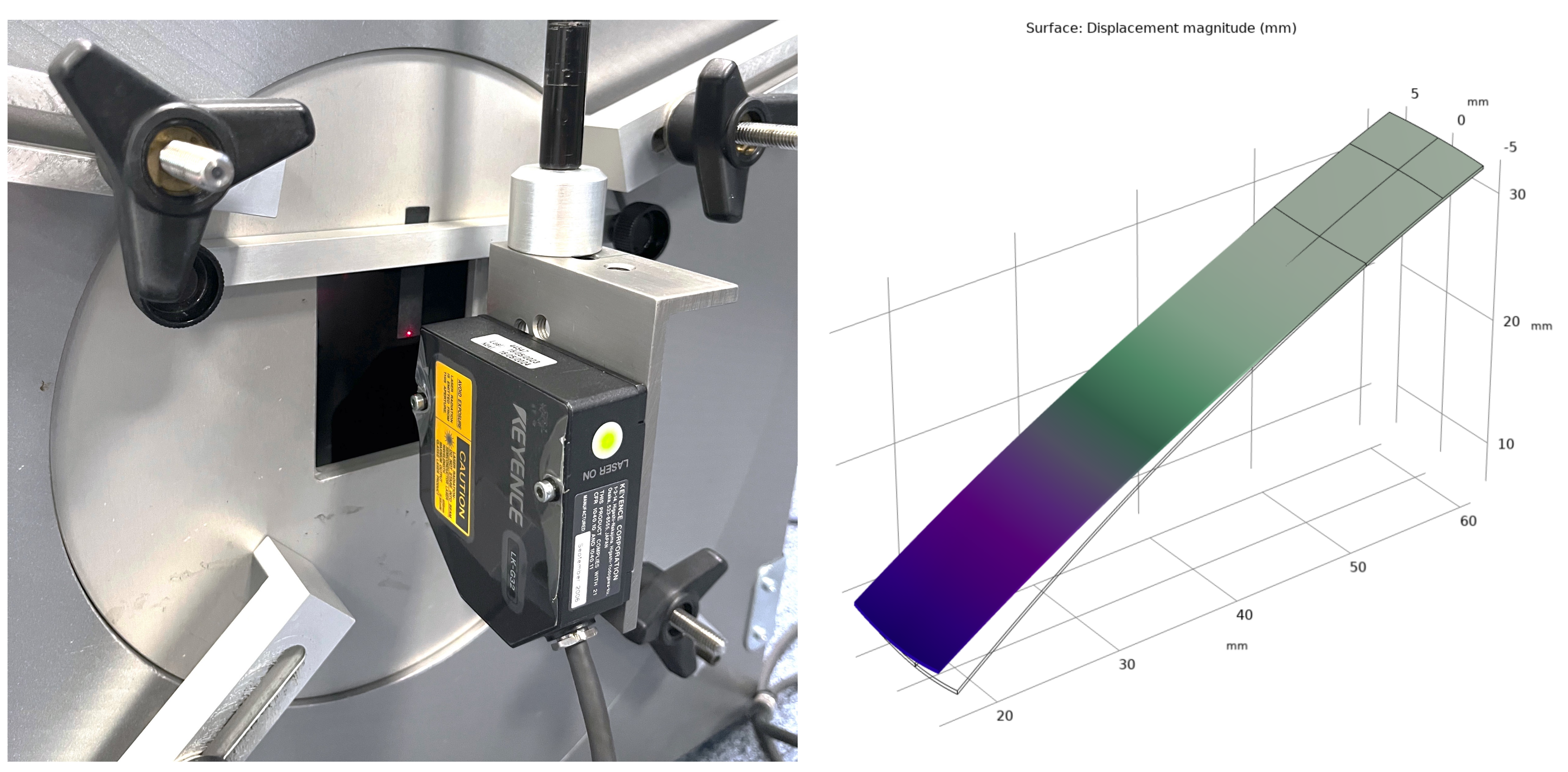

Left: The MPM measurement bench set up for cone material excitation. **Right**: Simulated excitation used to obtain the material's Young's modulus.

Methodology

The process began with physical testing of materials using Klippel Material Parameter Measurement (MPM) module to determine their resonance frequencies. These measurements were coupled with FEM simulations to estimate the Young's modulus for each material.

After evaluating material properties, three loudspeakers were assembled. A detailed FEM model was created for each loudspeaker.

Finally, the simulations were compared with physical measurements of frequency response and impedance curves, as well as observing deformations at specific frequencies utilizing Klippel Scanning (SCN) module, allowing for a robust comparison between the modeled and actual performance.

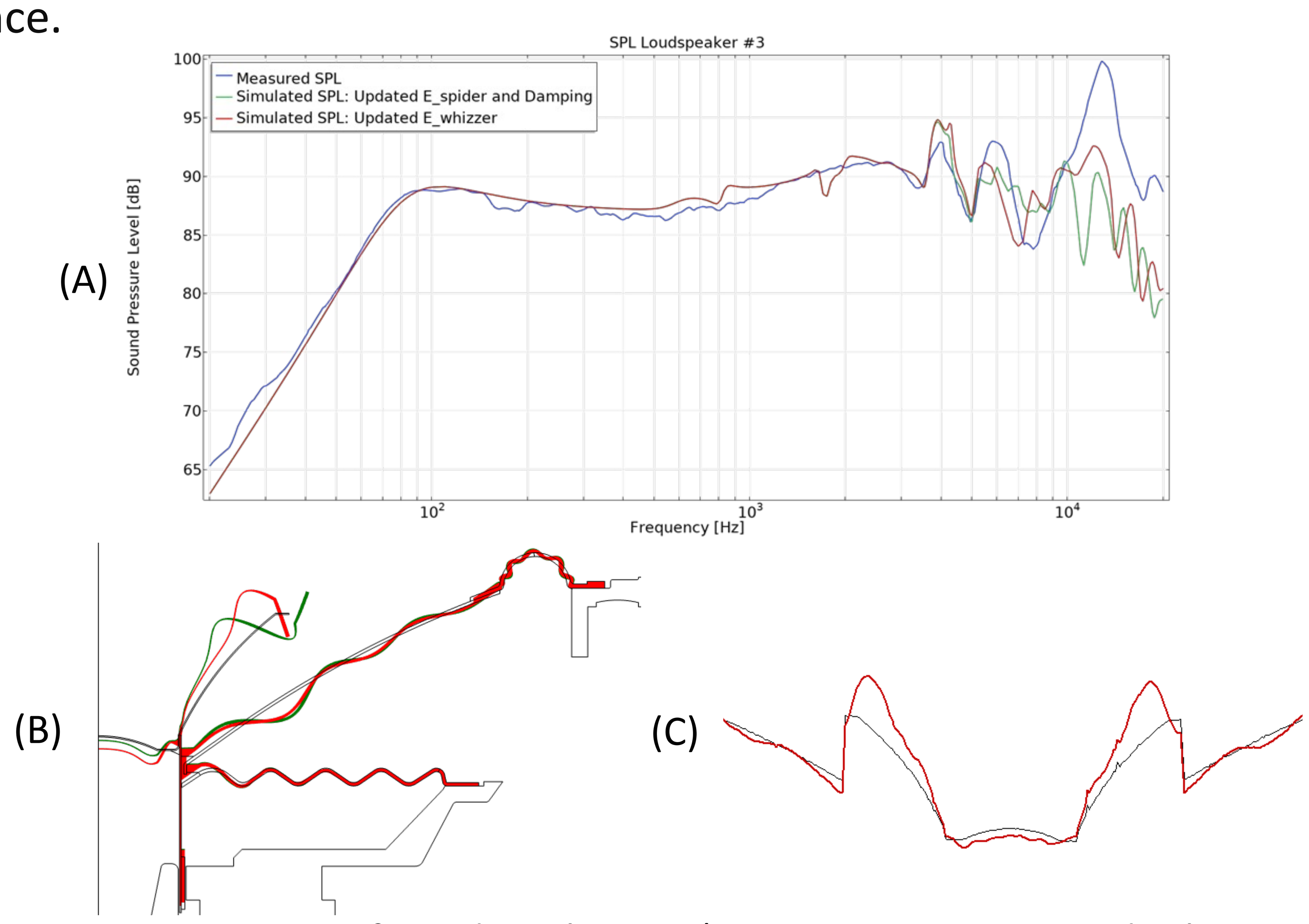

(A) Frequency response of Loudspeaker #3 (paper + mica cone and whizzer, foam surround) displaying change in whizzer Young's modulus. **(B)** Simulated deformation at 12 kHz displaying the effect of this change. **(C)** Measured SCN of actual speaker whizzer deformation at 12kHz.

Results

The comparison between simulated and measured loudspeaker performance showed a strong alignment. However, some discrepancies at higher frequencies were attributed to variations in material properties. One significant observation was the frequency-dependent behavior of the Young's modulus in fiberglass cones. Another observation made can be seen by comparing Figure B (Green) simulated whizzer deformation, with actual deformations (Figure C). By increasing the Young's modulus of the whizzer material, a better matching of real-life behaviors was made (Figure B, Red). This is much easier observed in animations.

Insights like these allow for more accurate modeling of loudspeaker materials and lay a foundation for future exploration of novel materials with enhanced acoustic properties and mechanical durability, guiding the development of more reliable and high-performance loudspeakers.

REFERENCES

1. Yamamoto et al. , "New Materials for Loudspeaker Diaphragms and Cones, an Overview", Pioneer Electronic Corporation, 1981.
2. W. Cardenas et al., "Optimal material parameter estimation by fitting finite element simulations to loudspeaker measurements," in AES Convention 144, 2018.
3. Klippel GmbH, "Material Parameter Measurement (MPM) Manual," Dresden, Germany, 2019.

faital ALPSALPINE ALPS ALPINE GROUP POLITECNICO DI MILANO 1863 Music and Acoustic Engineering

Guidelines

General Notes for Using the Template

- Do not adjust the template; work within it. See the examples provided.
- Left align text within textboxes, and do not justify your text.
- Titles are the largest font on the slide (90–120 pt.), then subtitles (70–80 pt.). Captions, references, and affiliation are the smallest text (18–40 pt.).
- Titles and subtitles are bold; any other use of bold should be for emphasis.
- Text is either black or grey and should only be adjusted for diagrams.
- Images can be adjusted and fitted into the boxes using the *Crop* feature. (In PowerPoint: *Format* tab → *Size* section on the right → *Crop*.)

Please keep in mind:
- **The solid red lines are the 3 mm that will be cut off during printing.**
- The dotted lines represent a small margin that may or may not be cut off during printing.

Exporting an Image for the Header

The settings shown on the right export the highest quality image with a transparent background.

The most important settings to use are the two outlined in pink. This will export an image that can be placed in the blue space of the header.

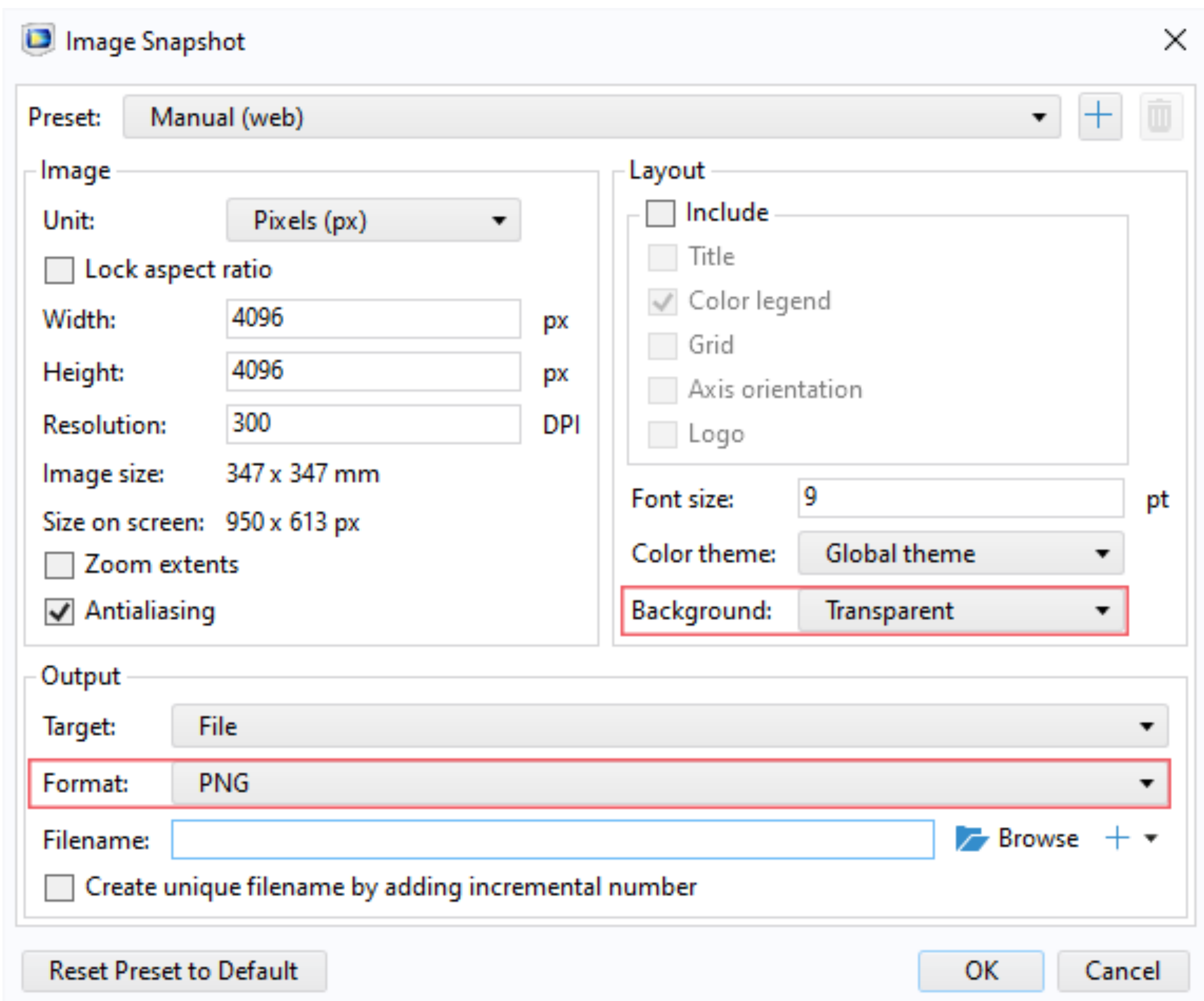

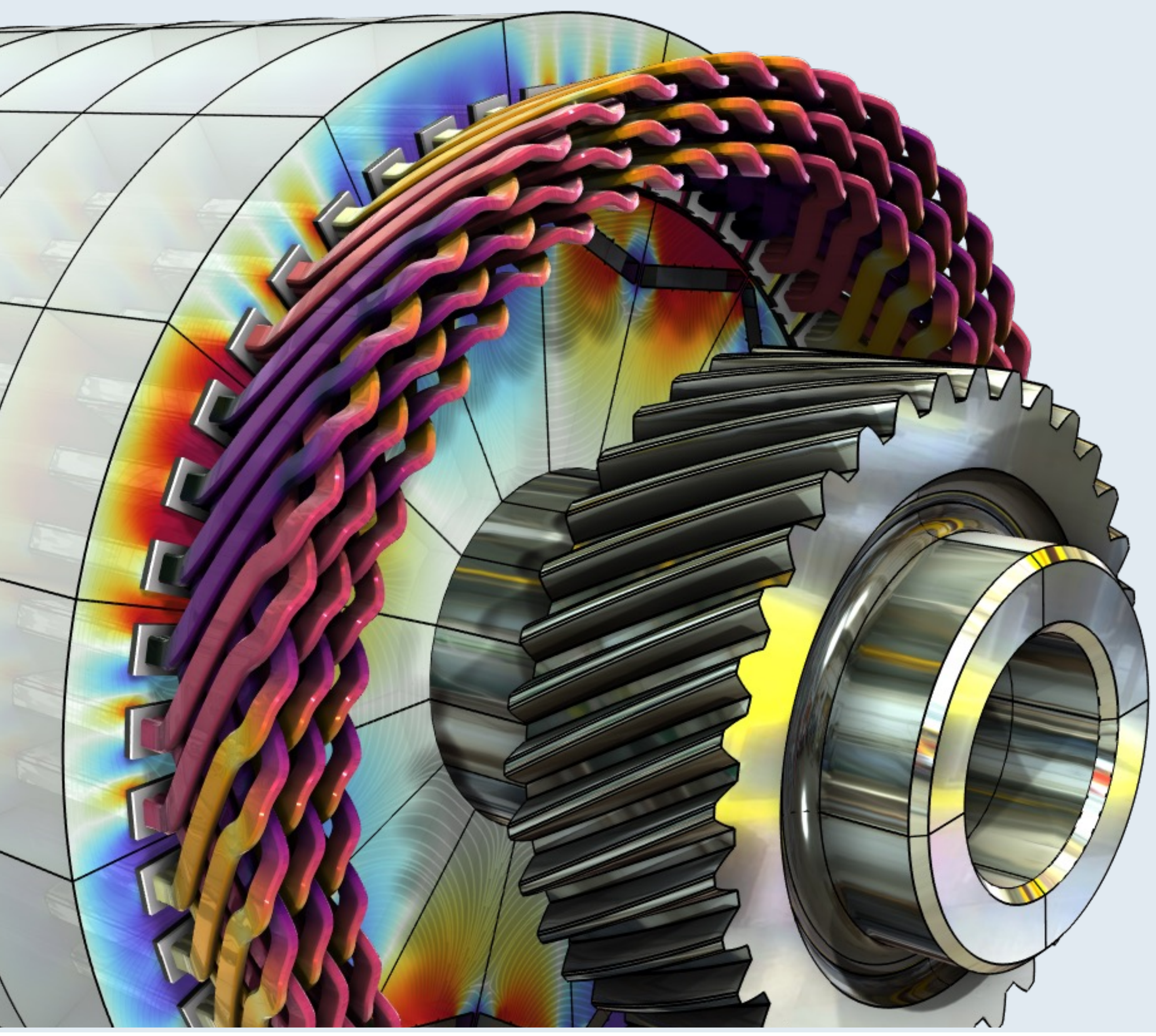

Analysis of a Permanent Magnet Motor in 3D

Optimize permanent magnet (PM) motor performance by understanding their full behavior, including sensitivity to high temperatures.

J. A. Smith[1], M. B. Smith[2]
1. Department (if applicable), Organization, City, Country.
2. Department (if applicable), Organization, City, Country.

Abstract

While PM motors are valued for the energy savings that they provide, there are some design limitations to address. For example, permanent magnets are sensitive to high temperatures. Such temperatures can occur when currents, particularly eddy currents, generate heat losses.

The findings offer greater insight into the behavior of PM motors, particularly by capturing the eddy current losses that occur within the magnets. This information serves as a useful resource for improving the design of PM motors, and therefore the technology they help power.

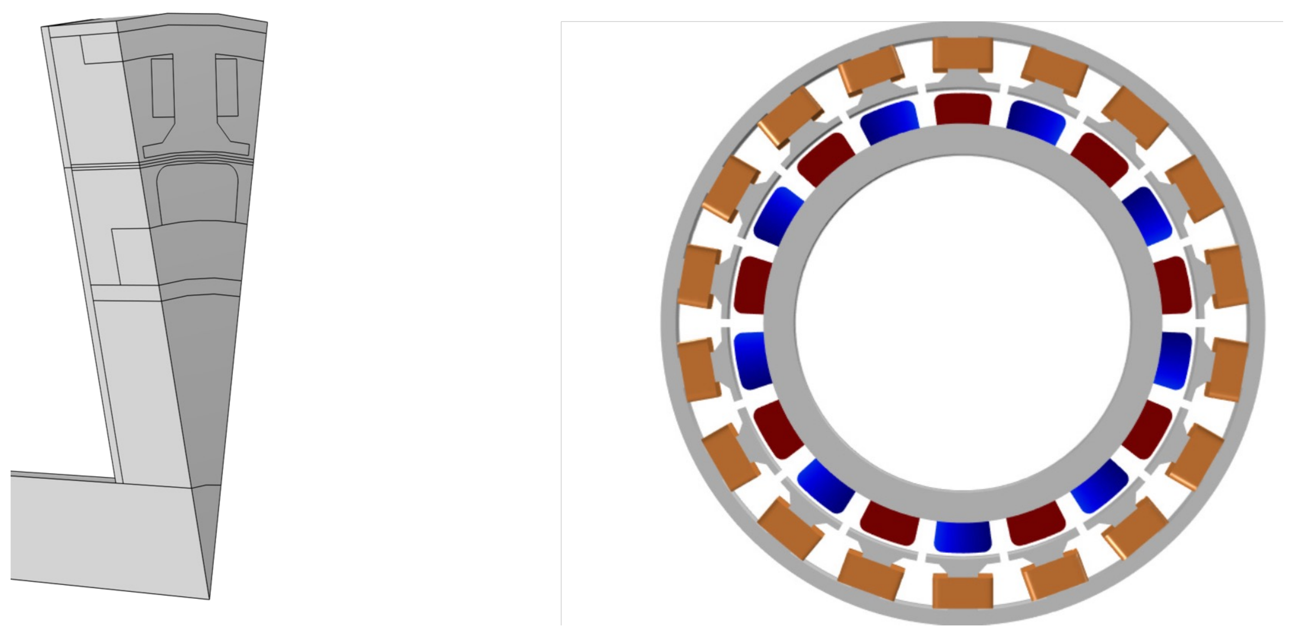

FIGURE 1. Left: Permanent motor sector. Right: Drawing of the PM motor.

Methodology

An 18-pole PM motor is modeled in 3D. Sector symmetry and axial mirror symmetry are utilized to reduce the computational effort while capturing the full 3D behavior of the device.

The conducting part of the rotor is modeled using Ampère's law:

$$\sigma\frac{\delta \boldsymbol{A}}{\delta t}+\nabla\times\left(\frac{1}{\mu}\nabla\times\boldsymbol{A}\right)=0$$

Results

The results can be seen in Figure 2, which shows the magnetic flux density for the motor in it's stationary state, that is, the initial conditions for the time-dependent simulation. In this state, the coil current is zero. It also shows the magnetic flux density for the motor after revolving one sector angle. In this plot, the air and coil domains are excluded in order to get a better view.

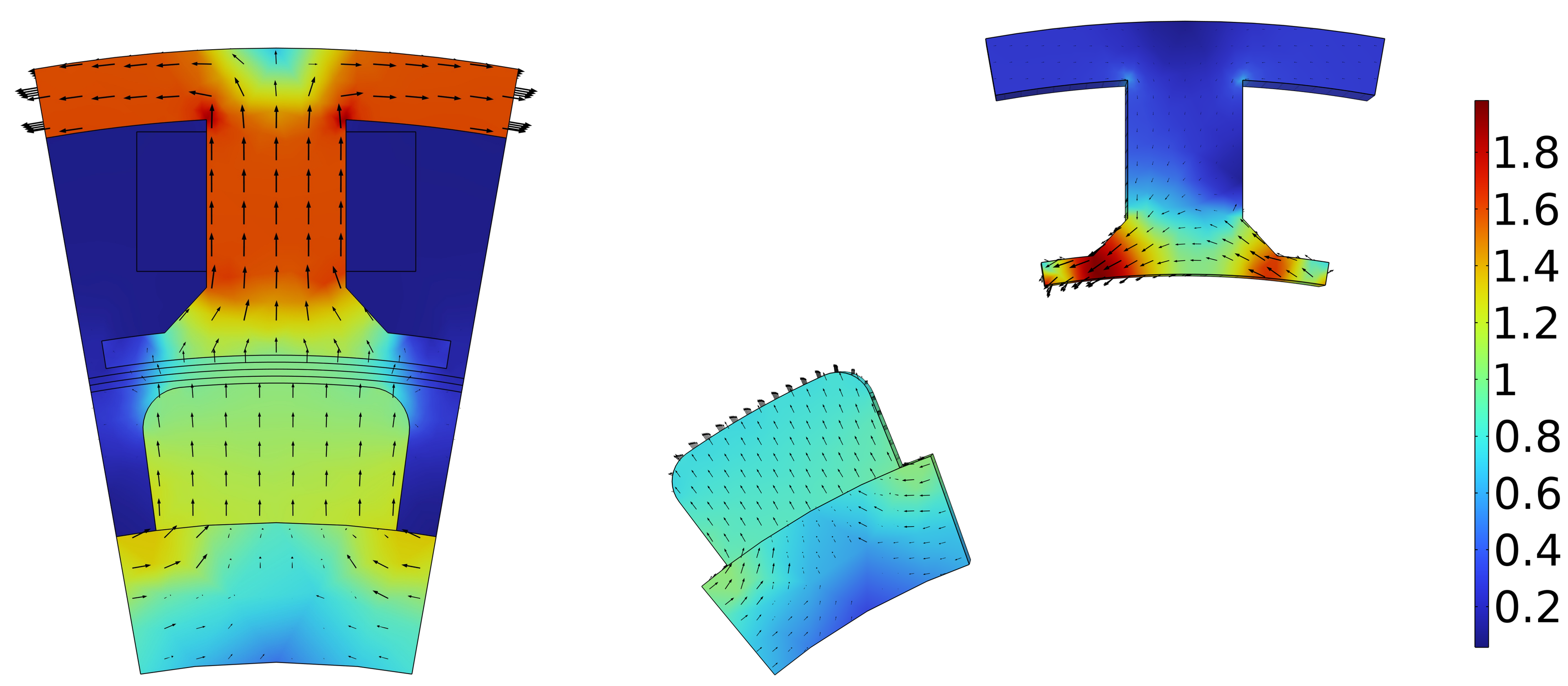

FIGURE 2. Left: Magnetic flux density from the permanent magnets with only the rotor at rest. Right: Magnetic flux density after revolving one sector angle.

REFERENCES

1. Author first initial and last name, "Article Title", *Journal*, Volume (vol.), Page numbers (pp.), Year.
2. Author first initial and last name, "Article Title", *Journal*, Volume (vol.), Page numbers (pp.), Year.
3. Author first initial and last name, "Article Title", *Journal*, Volume (vol.), Page numbers (pp.), Year.

COMSOL

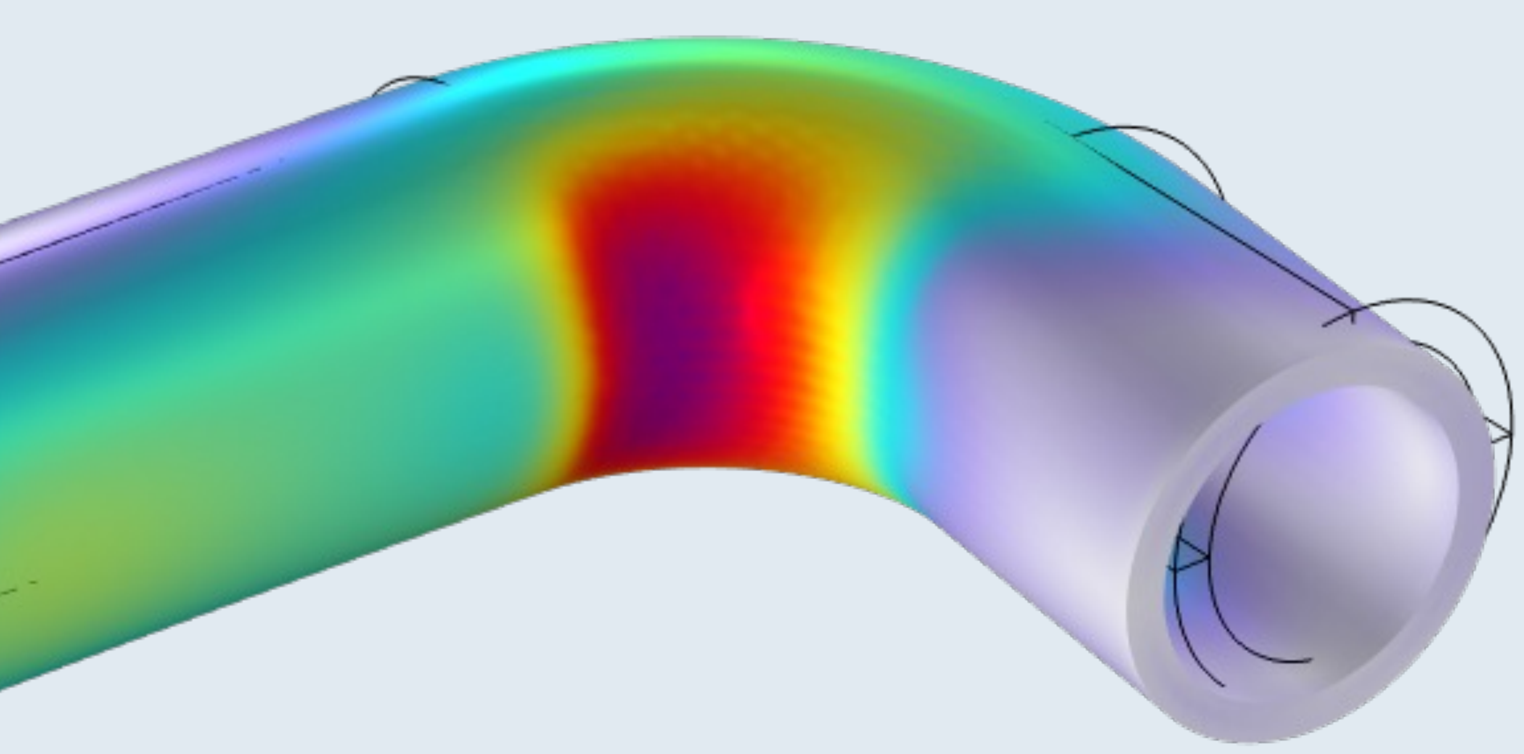

The Intriguing Stresses in Pipe Bends

For many structural engineers, beam theory is a popular analysis tool. Using the equations can be beneficial when considering structural behavior, as they are easy to apply and provide useful results. This work investigates one such case.

J. A. Smith[1], M. B. Smith[2]
1. Department (if applicable), Organization, City, Country.
2. Department (if applicable), Organization, City, Country.

Introduction & Goals

Pipe bends are common in piping systems, which typically transport liquids or gas, often under high pressure. One place where you may find a lot of pipes are oil tankers. The labyrinthine piping systems can look pretty fascinating.

Many piping standards (or codes) used for industrial applications are based on beam theory when it comes to the structural analysis. But, as we have already discovered, pipe bends generally do not behave like beams. When digging into piping standards, you will find a lot of information dedicated to pipe bends. In particular, piping standards recommend to apply correction factors to the stiffness and stresses for curved pipe sections. (Ref. 1)

FIGURE 1. Piping systems on an oil/chemical tanker. Image licensed under CC BY-SA 3.0 via Wikimedia Commons.

Methodology

The pipe is slender with a constant cross section, so it would seem like a natural choice to treat such a structure as a beam in a simplified analysis. The bending moment is the only load acting on the structure, and it's thus constant for any given section along the entire beam axis.

The maximum stress even occurs on the *inside* of the pipe. The cross section of the bend also deforms significantly, and, more specifically, it ovalizes with the major axis either being oriented in the bend plane or perpendicular to it depending on the direction of the bending moment.

Results

At a relative thickness of $t/R_0 \approx 35\%$ (which for any real application would be considered very thick), the stress distribution starts to change quite significantly. Additional perpendicular tensional stresses superpose the beam solution at the inner- and outer-bend radii.

Simultaneously, the top and bottom of the pipe show compressional stresses. These additional circumferential stresses arise due to the ovalization of the cross section. Ordinary beam theory explicitly ignores such cross-sectional deformations, and it does fall short in capturing its effect.

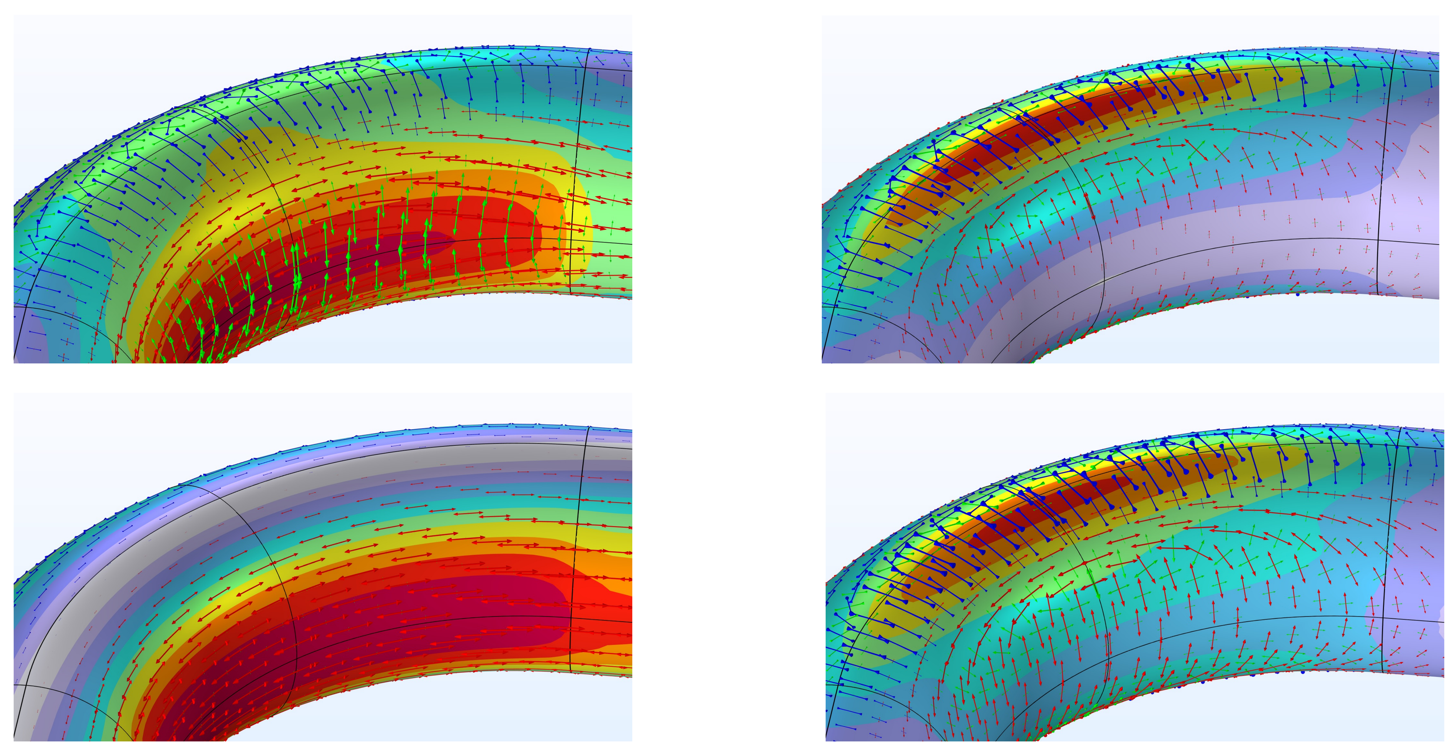

FIGURE 2. View of the pipe bend showing the von Mises stress (normalized) and principal stresses for different wall thicknesses.

REFERENCES

1. E.A. Wais and E.C. Rodabaugh, "Background of SIFs and Stress Indices for Moment Loadings of Piping Components", United States, 2005; https://www.osti.gov/biblio/841246
2. "Stress Intensification Factors (i-Factors), Flexibility Factors (k-Factors), and Their Determination for Metallic Piping Components", ASME, 2017; https://www.asme.org/codes-standards/find-codes-standards/b31j-stress-intensification-factors-flexibility-factors-determination-metallic-piping-components/2017/drm-enabled-pdf